JACS
JOURNAL OF THE AMERICAN CHEMICAL SOCIETY
Article
pubs.acs.org/JACS

Origin of Dark-Channel X-ray Fluorescence from Transition-Metal Ions in Water

Robert Seidel,[†] Samira Ghadimi,[†] Kathrin M. Lange,[†] Sébastien Bonhommeau,[‡] Mikhail A. Soldatov,[†,§] Ronny Golnak,[†] Alexander Kothe,[†] René Könnecke,[†] Alexander Soldatov,[†] Stephan Thürmer,[†] Bernd Winter,*[,†] and Emad F. Aziz*[,†,∥]

[†]Helmholtz-Zentrum Berlin für Materialien und Energie, Albert-Einstein-Strasse 15, D-12489 Berlin, Germany

[‡]Institut des Sciences Moléculaires, UMR 5255 CNRS, Université Bordeaux 1, 351 cours de la Libération, 33405 Talence Cedex, France

[§]Research Center for Nanoscale Structure of Matter, Southern Federal University, Sorge 5, Rostov-na-Donu 344090, Russia

[∥]Freie Universität Berlin, FB Physik, Arnimallee 14, D-14195 Berlin, Germany

Supporting Information

ABSTRACT: The nonradiative dark channels in the L-edge fluorescence spectra from transition-metal aqueous solution identify the ultrafast charge-transfer processes playing an important role in many biological and chemical systems. Yet, the exact origin of such spectral dips with respect to the X-ray transmission spectrum has remained unclear. In the present study we explore the nature of the underlying decay mechanism of 2p core-excited Co^{2+} in water by probing the nonradiative Auger-type electron emission channel using photoelectron spectroscopy from a liquid microjet. Our measurements demonstrate unequivocally that metal-to-water charge transfer quenches fluorescence and will inevitably lead to a dip in the total-fluorescence-yield X-ray absorption spectrum. This is directly revealed from the resonant enhancement of valence signal intensity arising from the interference of two identical final states created by a direct and Auger-electron emission, respectively.

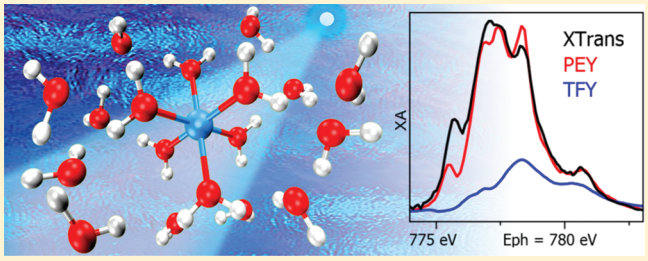

INTRODUCTION

Fluorescence yield (FY) L-edge X-ray absorption (XA) spectra from aqueous solutions have been reported previously,[1,2] and their usefulness for characterizing ultrafast charge-transfer processes in aqueous solutions of transition-metal (TM) ions in water has been suggested. However, all those XA measurements were based on detection of either the total fluorescence-yield (TFY) or the total electron-yield (TEY),[1,3] which can be relatively easily performed. Such total-yield studies are not conclusive, though, providing no direct and quantitative information on the electronic relaxation pathway of the 2p-core excited TM ion in aqueous solution (ion(aq)), and furthermore, total-yield XA spectra cannot be accurately interpreted without additional electronic-structure information or theoretical modeling.[4,5] A crucial issue with obtaining XA spectra other than by transmission measurements is that secondary processes connected with the electronic relaxation may be state-dependent, and for instance, the probability for the refill of the 2p core-hole by a metal-derived 3d valence electron can vary. Such effects, primarily caused by charge and energy (e.g., of the type intermolecular Coulombic decay, ICD[6,7] transfers) would be seen in both the fluorescence and the electron spectra, but the behavior is not necessarily the same, as we will show here for Co^{2+} aqueous solution. In this situation, the FY-XA intensity cannot be assumed to be proportional to the number of the core holes created by X-rays (where we implicitly assume prompt refill by valence electrons). And yet the comparison between the true transmission (Trans) XA spectrum, where there are no disturbing de-excitation processes to be taken into account, and the decay (radiative or nonradiative) spectra turns out to be extremely useful. The spectral differences provide important insight into the ultrafast electron dynamics which occur on the few-femtosecond time scale of the core-hole lifetime. And yet, this information is hardly accessible from total-yield measurements, as we have already mentioned. Instead, explicit tracking of charge transfer from the metal to the ligand (MLCT) or the reverse (LMCT) would require an energy- and state-resolved spectroscopy measurement which allows for exploration of the actual de-excitation channels, with access to the TM-derived 3d-valence and 2p-core energies of the initial and final electronic states of the aqueous solution. This is accomplished by a combination of off-resonant and resonant photoelectron (RPE) spectroscopy, applied to a vacuum liquid microjet.[8,9]

Received: August 22, 2011
Published: December 16, 2011

dx.doi.org/10.1021/ja207931r | J. Am. Chem.Soc. 2012, 134, 1600−1605

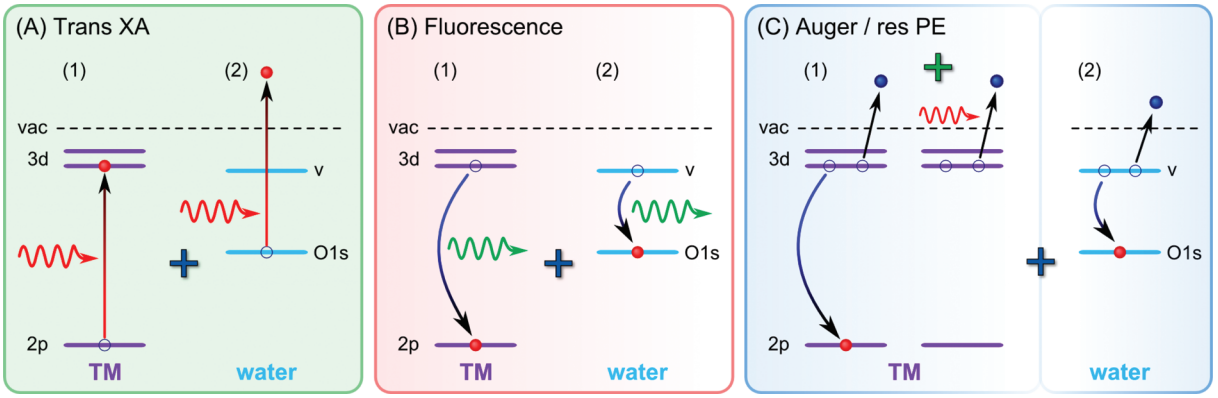

Figure 1. Illustration of the X-ray absorption process (A) and subsequent fluorescence- (B) and electron-emission (C) decays, occurring in TM-ion aqueous solution at the metal 2p threshold.

Before presenting our measurements, we would like to familiarize ourselves with the complexity of the "fluorescence dip" phenomenon in light of the different spectroscopic methods applied here. A true X-ray absorption measurement detects the fraction of photons absorbed by the sample; second-order processes are thus irrelevant. Figure 1A depicts an energy-level scheme illustrating absorption/transmission, i.e., the 2p−3d electron promotion at the resonance energy (left), and the O1s ionization of H_2O(aq) (right). For Co^{2+} aqueous solution, both processes occur at 776−800 eV photon energy (the L-edge energy range of Co^{2+}); the water ionization energy is 538.1 eV.[10] Figure 1B illustrates the subsequent (∼1% minority) fluorescence decay. It shows the refill of the 2p core-hole by a 3d electron, with the released energy being carried away by an X-ray photon (left), which in our experiment is detected by a photodiode (TFY). Analogous processes will occur for H_2O(aq), with the difference though that core refill follows ionization of water (right). Given the approximately 50:1 number-ratio of H_2O molecules to Co^{2+} cations for the concentrations used, the solute fluorescence signal will be measured on top of a broad fluorescence-signal background from water, which contributes at any energy in that range. The latter is due to elastically scattered light emitted by the solvent. A dip, or disappearance of peaks in the TFY-XA spectrum would hence be the net result of solute and solvent contributions, but relative weights are not trivial to determine. We show in the present study that the solute contribution can in part be identified by RPE spectroscopy measurements, probing the ultrafast nonradiative de-excitation channel, on the lifetime of the core hole; see the sketch of Figure 1C. Because of hybridization between water and metal 3d energy levels, the valence signal will be considerably enhanced as a consequence of the coherent interference of two identical final states.[8] One is reached by direct emission of a photoelectron (direct ionization), and the other results from second-order electron emission, by an Auger-type process. Both processes are indistinguishable (Figure 1C, left). For completeness, we also sketch the Auger decay for water(aq) (Figure 1C, right), but that process will not be analyzed in the present study.

We notice that the interpretation of XA spectra from aqueous TM solutions, often based on ligand-field multiplet (LFM) theory,[4,5] is certainly an interesting *atomic* approach, in the absence of further experimental data. LFM calculations do provide an idea of formal charge transfer, without taking into account the explicit bonding interaction between metal ion and water, though, which however is the key to charge and energy transfers.

■ EXPERIMENTAL SECTION

All studies were conducted with tunable soft-X-ray photons provided from the U41 PGM undulator beamline of the synchrotron-light facility BESSY II, Berlin. Experimental details have been described previously.[11−13] Shortly, photoemission measurements were performed from a 20-μm sized liquid vacuum jet. The jet velocity was approximately 80 ms^{-1}, and the jet temperature was 6 °C. Electrons were detected normal to both the synchrotron-light polarization vector and the flow of the liquid jet. Photoelectrons pass through a 100-μm diameter orifice which separates the main interaction chamber (operating at 10^{-5} mbar) from the differentially pumped detector chamber (operating at 10^{-9} mbar) housing a hemispherical electron energy-analyzer equipped with a multichannel detector. The orifice is at approximately 0.5 mm distance from the liquid jet—a short enough distance to ensure that detected electrons have not suffered from inelastic scattering with water gas-phase molecules around the small sized liquid jet. The energy resolution of the U41 beamline is better than 350 meV at the incident photon energies used here, and the resolution of the hemispherical analyzer is constant with kinetic energy of about 200 meV, at 20 eV pass energy. The small focus size, 23 × 12 μm^2, of the incident photon beam allows for matching spatial overlap with the liquid microjet, reducing the gas-phase contributions of the measured spectra to less than 5%.

Trans- and TFY-XA measurements were performed using a cell with two Si_3N_4 membranes (150-nm thickness and 2-μm spaced) and a flow cell (with a speed of ∼100 mL/min behind a Si_3N_4 membrane), respectively. In previous comparative test measurements, it was shown that spectra are identical when using a free liquid jet.[14] Measurements from aqueous ionic solution are thus not affected by the window.

The aqueous solutions were prepared using deionized water, and the $CoCl_2$ hexahydrate salt was of >99% purity (Sigma Aldrich). Concentrations of 0.25 *molal* (m), 0.5 m, 1 molar (M), and 1.5 m were studied here, although our focus is on 1 M and 1.5 m. The 1.5 m solution is slightly lower in concentration, 0.85 M, and this small difference should not affect our comparison of fluorescence and electron emission. Importantly, though, at this concentration, approximately half of the complexes have a first solvation shell with one water ligand substituted by a Cl^- ion, i.e. $CoCl(H_2O)_5^{1+}$. Implications of such speciation will be addressed below. Co^{3+} configurations are not stable in water and will not be considered.

■ RESULTS AND DISCUSSIONS

Figure 2 presents L_3 ($2p_{3/2}$) and L_2 ($2p_{1/2}$) edge XA spectra from 1 M $CoCl_2$ aqueous solution, measured by partial-electron yield (PEY) (A), transmission (A and B), and TFY (C). The PEY results from signal integration of the valence PE spectra

dx.doi.org/10.1021/ja207931r | J. Am. Chem.Soc. 2012, 134, 1600−1605

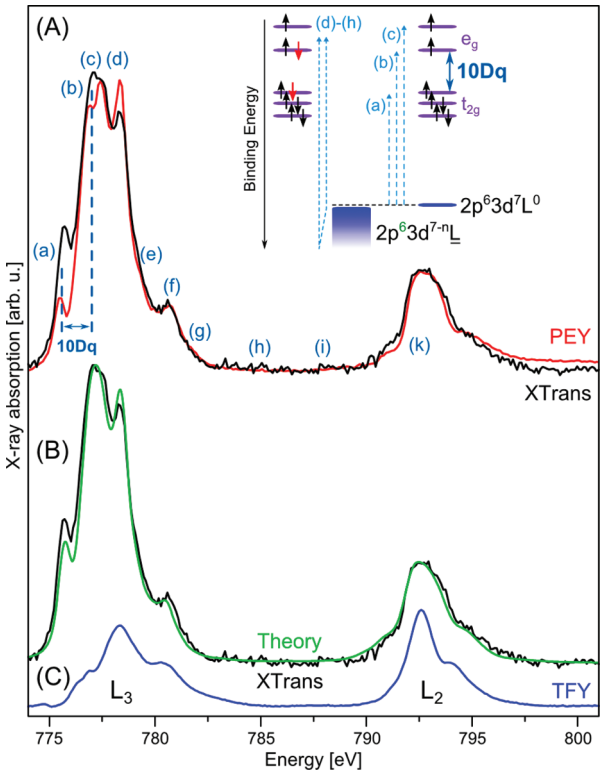

Figure 2. PEY (A), transmission (A and B), and TFY (C) XA spectra from $CoCl_2$ aqueous solutions obtained at the Co 2p threshold (L-edge). Concentrations are 1.5 m (~ 0.85 M) (A), 1 M (B), and 1 M (C).

(5−40 eV binding energy range) when sweeping the photon energy across the Co^{2+} $2p_{3/2}$ and $2p_{1/2}$ absorption; the actual individual RPE spectra recorded at a given photon energy will be discussed later. Trace B also displays the calculated XA spectrum using LFT theory. As aforementioned, because of rigorous parametrization of charge transfer, agreement with experiment can be very good. In fact, experimental spectra, including peak (a), are reproduced best when explicitly allowing for MLCT; the specific parameters used in our calculations are presented in the Supporting Information. Small discrepancies between experimental and calculated spectra probably arise from minor distortions of the octahedral configuration due to the two species present in the solution ($Co(H_2O)_6$ and $CoCl(H_2O)_5$).[3] Spectral intensities in Figure 2 are displayed as to yield identical heights of the L_2 peaks, which have a rather similar shape in all spectra. For the Trans- and PEY-XA measurements, even the L_3-edge data are remarkably similar, implying that the decay of the excited electron is nearly quantitatively captured in the PEY-XA spectra. The electron signal is thus primarily connected with the relaxation of the excited electron (through 2p core-hole refill), rather than with the decay of any other 3d-electron. RPE spectroscopy, at least for the particular TM(aq) of this study, thus turns out to be a rather fine method for obtaining undisturbed L-edge XA spectra. Even though photon-out techniques probe far deeper into the solution due to much different attenuation of photons as compared to electrons, the current PE measurements are primarily sensitive to the bulk solution as well. As was shown in several previous depth-dependent PE studies from aqueous solution, (photo)electron kinetic energies when larger than approximately 600 eV, reproduce bulk solution properties. Of course, one still probes very near the interface, and yet deep enough, just reaching bulk structure. For instance, nitrogen 1s PE measurements from nitric acid solution accurately reproduce the degree of dissociation of HNO_3 of bulk solution when using 600-eV electrons, while considerably less dissociation is observed for surface probing, then using 100 eV electrons.[15,16] Since the RPE spectra of the present work are detected at electron kinetic energies above 700 eV, it is no surprise that the Trans XA and PEY-XA of Figure 2 agree so well, and importantly, surface-specific speciation will play no role here. But when comparing spectral differences for the two methods, and considering that experiments were conducted with completely different setups, one would expect to observe some smaller differences, within the experimental reproducibility. In our case, this probably explains small intensity differences for peaks (b) and (d). But the observed effect for peak (a) seems too large and deserves our special attention. The lower intensity of this peak in the PEY-XA spectrum is a qualitative indication of aforementioned second-order decay effects, hinting at the distinctly different relaxation of the state that is excited at 775.5 eV (see below). We would like to point out that the overall lower L_3 intensity of the TFY-XA spectrum can be attributed to the fact that fluorescence is the minority channel, and rate-changes will be picked up more sensitively and hence changes will be larger, as compared to the case of electron channels. When interpreting TFY-XA spectra, one must thoroughly account for possible saturation effects, though. This was done in two of our previous studies,[3,17] where we found that, for 1 M (1: 55.5 in water), concentration saturation effects are negligible compared to the strong intensity decrease of the L_3-edge relative to L_2-edge in our spectra. The reason why the L_2-edge spectrum exhibits almost negligible changes but the intensities of the L_3-edge spectrum change so much for the different techniques is the shorter lifetime of the $2p_{1/2}$ core hole, ~0.6 fs, as compared to ~3 fs for $2p_{3/2}$.[18] Hence, the preference for the nonradiative (delocalized) over the radiative (local) $2p_{3/2}$ decay indicates that the electron delocalization time required for the former process is faster than 3 fs but slower than 0.6 fs. Note that the negligible change in the L_2-edge spectra is the main reason for using its spectral intensity for normalization. An interesting detail, reminding of the TFY-dip in the measurements from Fe^{3+} aqueous solution,[1] is the occurrence of a small dip in the TFY-XA spectrum of Figure 2C, exactly coinciding with the energy position of peak (a). As discussed along the lines with Figure 1, such a dip can arise if the solute signal is quenched below the level of water emission. To see if that does indeed hold for Co^{2+}(aq), we must explore the origin of the strikingly lower intensity at peak (a) for PEY than for Trans XA. Here the off-resonant PE and the explicit RPE spectra come into play.

Figure 3A shows the valence PE spectrum from 0.25 m $CoCl_2$ aqueous solution, recorded at a photon energy of 200 eV. Electron energies are displayed as binding energies (BE), calibrated by the $1b_1$ energy of liquid water,[19] and referenced to vacuum. The other spectrum, in black, is that from 0.5 m NaCl aqueous solution (yielding identical chloride concentration), obtained under identical experimental conditions. This comparison is necessary for determining the BEs of the partially occupied metal-derived 3d states because their PE spectrum overlaps with the emission from the 3p orbitals of the Cl^-(aq) counteranion. Subtraction of the alkali-halide(aq) spectrum from the $CoCl_2$(aq) spectrum (yielding the differential spectrum, in green) reveals that the lowest ionization of

dx.doi.org/10.1021/ja207931r | J. Am. Chem.Soc. 2012, 134, 1600−1605

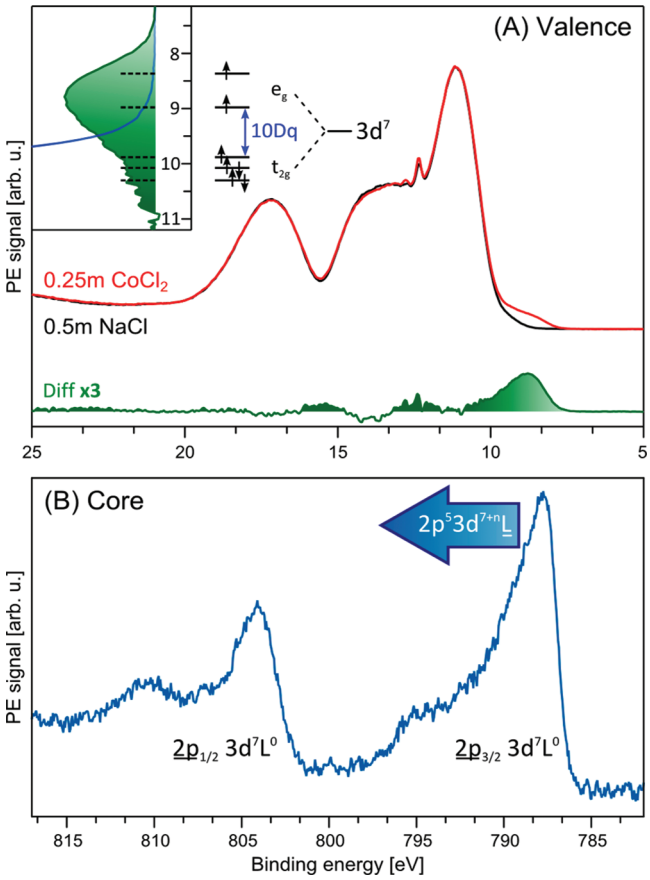

Figure 3. (A) Off-resonant valence PE spectrum from 0.25 m $CoCl_2$ aqueous solution (in red), measured at 200 eV photon energy. The black spectrum is from 0.5 m NaCl aqueous solution and was measured under the same conditions. The difference spectrum (in green) identifies Co-derived states. Inset: Comparison of the experimental low-BE PE peak with the e_g and t_{2g} states as expected for $3d^7$ energy-level splitting in an octahedral ligand field. See main text and Table 1 for the explicit energy values. (B) 2p core-level PE spectrum from 0.5 m $CoCl_2$ aqueous solution measured at 920 eV photon energy.

the solution is from the metal complex. This is evidenced by the positive signal at lowest BEs, extending from 8 to 10 eV, which is well below the onset for ionizing neat liquid water. That signal contains contributions from several 3d-derived $Co^{2+}(aq)$ states, which stay unresolved though because of the ~1-eV broad energy distributions from different hydration configurations. But we can fairly accurately estimate the center energies from the onset of the PE emission and from the principle level splitting in the octahedral ligand field resulting from the surrounding water-oxygen. In octahedral symmetry, the $3d^7$ level (ground-state configuration of Co^{2+}) splits into e_g (doublet) and t_{2g} (triplet) levels with energy separation defined as 10Dq. The $Co^{2+}(aq)$ complex is known to assume a high-spin ground-state configuration, which is a consequence of the spin-pairing energy being larger than 10Dq. Comparison with experiment (see inset of Figure 3A) shows reasonably good agreement, and the somewhat too low signal of the experimental peak at the t_{2g} energies probably results from slight overestimation of the emission signal from 3p orbitals of $Cl^-(aq)$ ions in the spectrum subtraction. Note that the e_g states have splitting in the energy level (peaks b and c in Figure 2A), which leads to a slight distortion for the octahedral symmetry. For simplicity, we will keep labeling these states as e_g. The actual values for the e_g energy spacing (0.7 eV) and for 10Dq (1.2 eV) used in the figure have been obtained from the PEY-XA spectrum (and will be explained below). Resulting BEs are presented in Table 1. We note that the 1.2-eV value for

Table 1. $Co^{2+}(aq)$ Energies Determined from Experiment, All Given in eV[a]

BE (eV)	t_{2g} 10.2	e_g 9.1	e_g 8.4
$2p^53d^7L^o$ 787.5	777.3	778.4	779.1
XA	775.5 (a)	776.7 (b)	777.4 (c)

[a]First row: Approximate valence energies of 3d-derived levels, from Figure 3. For simplicity we have maintained the terms "e_g" to indicate that these levels are e_g-derived energy-split in the octahedral ligand field. Second row: Calculated energy differences between valence energies and the energy of the $2p_{3/2}$ unscreened level (at 787.5 eV, from Figure 3B). Third row: Photon energies corresponding to peaks (a)−(c) in the PEY-XA spectrum (Figure 2C).

10Dq is in good agreement with our LFT theory calculations, yielding 1.1 eV (see Table S1 of the Supporting Information). Probably the most important finding from our valence-spectrum analysis is that metal t_{2g} levels overlap energetically well with the valence band of water, enabling strong orbital mixing, in agreement with previous density-functional theory (DFT) calculations.[20] Orbital overlap also plays an important role in the excited state and explains the different relaxation behavior for pre-edge excitation (peak (a)), as we will see.

Figure 3B presents Co^{2+} $2p_{3/2,1/2}$ core-level PE spectra from the same $CoCl_2$ aqueous solution, but measured at 920 eV photon energy. Similarly to the case of crystalline CoO,[21,22] spectra are dominated by electronic multiplet and screening effects associated with the core hole produced in the photoemission process. The former contributions are responsible for the large energy tail (extending over more than 10 eV) at the high-BE side of the main $2p_{3/2,1/2}$ peaks. Studies from solid CoO[21,22] would suggest that the main peak at 787.5 eV BE is due to the $\underline{2p}_{3/2}{}^5 3d^7L^o$ unscreened final state. Here L^o denotes zero charge transfer from the water ligand; $\underline{L}$ and L^{-n} will then refer to LMCT and MLCT, respectively. Distinct electronically screened cobalt 2p-states, $\underline{2p}_{3/2}{}^5 3d^{7+n}\underline{L}$, barely exist in the spectrum of Figure 3B, except for the small satellite peak at 794.5 eV BE. The latter most likely corresponds to maximum charge transfer, possibly with charge increase $n > 1$. Fractional-charge states probably contribute to the broad sloping PE signal of the multiplet states. Analogous observations can be made for the $2p_{1/2}$ PE peak.

In an attempt to correlate specific 2p−3d transitions with the peaks of the XA spectra (Figure 2), we calculate the respective differences between core and valence BEs, from Figure 3. Values are presented in Table 1. Apparently, the three lowest-energy XA transitions, XA peaks (a), (b), and (c), can be associated with the main PE peak and the corresponding excitations into the only one-half-filled t_{2g} state and into the two e_g states, respectively. Absolute binding energies and transitions are depicted in the energy-level diagram shown in the inset of Figure 2, tier A. Due to final-state effects, the calculated BE differences are approximately 1.7 eV larger than those inferred from the respective energies of the XA spectrum (see Table 1). Values for the e_g-level splitting, and those for 10Dq can be thus inferred from the energy differences between peaks (c), (b) and between peaks (b), (a), respectively. This

dx.doi.org/10.1021/ja207931r | J. Am. Chem.Soc. 2012, 134, 1600−1605

information was already anticipated when discussing the 3d-derived valence PE spectrum from Co^{2+}(aq) along with Figure 3A. Higher-energy peaks in the XA spectrum (Figure 2, (d)–(g)) then identify 2p–3d transitions connected with the 2p-PE peak at higher BE. The observed different intensities of peaks (a), (b), and (c) of the Trans XA spectrum reflect different cross sections for excitation into different d states (see above). But judged from the yet lower signal intensity of peak (a) in the PEY-XA spectrum, there must be additional effects at play, causing some quenching of the fluorescence channel. Unlike for all other excitation energies where the excited electron readily relaxes by a very similar mechanism, the electron excited into t_{2g} appears to relax by some different path. This is indeed corroborated by the 2p RPE valence spectra from $CoCl_2$ aqueous solution but requires more detailed spectral analysis to be revealed and will be explored next.

The following is an analysis of the actual RPE valence spectra, which when summed up yields the PEY-XA spectrum (of Figure 2, tier A). Figure 4 shows a series of spectra from 1.5 m $CoCl_2$ aqueous solution, obtained at photon energies corresponding to the characteristic L_3-XA energies. PE intensities are displayed as measured, and changes of the photon flux have been taken into account. At photon energy slightly below the L_3-edge absorption onset (represented here for the 773 eV photon energy), we obtain the direct PE spectrum from the solution, which is similar to the spectrum of Figure 3A, where we have used the 200 eV photon energy. Differences in relative intensities for the two measurements essentially arise from different photoionization cross section changes. When raising the photon energy, and each time a resonance is excited, the valence-signal intensity in the 8–22 eV region increases. The origin of this enhancement is the aforementioned superposition of an (super-Coster–Kronig) Auger decay and the direct PE channel (see Figure 1C). One can identify Auger electron emission in the off-resonant PE spectra, i.e., when the photon energy is larger than the 2p ionization energy. This is demonstrated in the top spectrum of Figure 4, for a photon energy of 805 eV. The broad Auger feature, containing contributions from Auger decay associated with both $2p_{3/2}$ and $2p_{1/2}$ core-hole refill, extends from 35 to 55 eV. Auger emission can still be seen when exciting at a photon energy of 792.4 eV, which is above the $2p_{3/2}$ ionization energy but below the $2p_{1/2}$ ionization threshold. On the BE scale used in Figure 4, the Auger peak is now centered near 28 eV. Then, when exciting at any $2p_{3/2}$ resonance, we find that valence intensities become maximal exactly at the extrapolated positions of the Auger emission. In fact, the small shift of peak maxima, highlighted here for the 777.4 eV photon (corresponding to XA peak (c)) and 778.4 eV (XA peak (d)) (see marked positions in Figure 4) is reminiscent of Auger-electron constant kinetic energy.

In search for a specific spectral signature of some unusual behavior when exciting at XA-peak (a), we take a closer look at the evolution of the RPE spectra as a function of photon energy. The inset of Figure 4 thus shows enlargements of the valence spectra measured at XA peaks (a), (c), (d), and (f), but this time all spectra have been normalized to yield the same height at the high BE tail. Scaling factors are indicated. Note that we have also subtracted the (off-resonant) 773-eV water spectrum (of main Figure 4, bottom tier). In the bottom trace of the inset figure, we reproduce the Co^{2+}(aq)-derived PE contributions (measured at off-resonant excitation, at 200 eV; from Figure 3A). This comparison nicely corroborates the

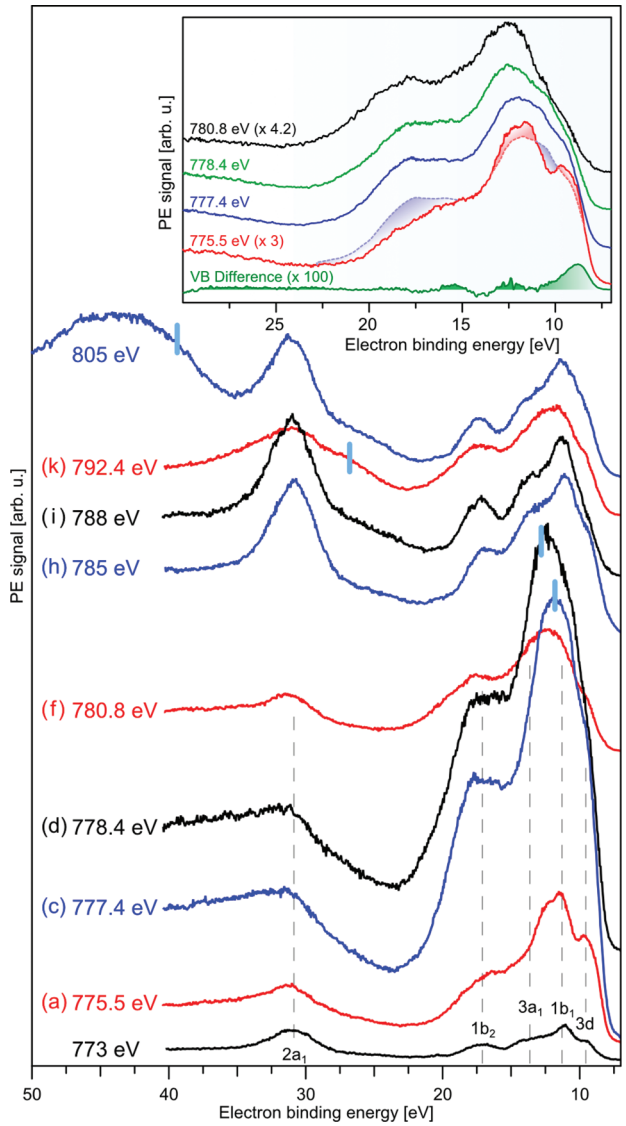

Figure 4. Valence RPE spectra from 1.5 m $CoCl_2$ aqueous solution measured at the Co^{2+} $2p_{3/2}$ threshold; explicit photon energies are indicated. Contributions from Auger-electrons are indicated by the blue bars. Notice that Auger peaks move on the binding-energy scale presented here.

nature of the signal enhancement, i.e., the interference of the direct Co^{2+}(aq)-ionization channel and the Auger-decay channel. Here we recall that Auger energies extend over a wide enough energy range to ensure overlap with the direct electron emission peaks from Co^{2+}(aq) (small peaks shown in green shade). Aside from the small Auger-peak shifts (already marked in the main figure), the top three spectra, corresponding to excitation at XA peaks (a), (b), (c), and (d), line up almost quantitatively. The one single remarkable difference is that for excitation at the lowest photon energy—peak (a)—the spectrum lacks noticeable intensity in the 16–22 eV energy range (indicated by the shaded area). This implies that all the higher-excited states relax by the same or similar mechanism, but the relaxation behavior of the $\underline{2p}t_{2g}^{6}$ state is different and can be explained together with the valence spectrum of Figure 3A. Above we have argued that lower intensity in the PEY than in the Trans-XA spectra is due to a smaller probability of a 3d electron to refill the 2p core hole,

dx.doi.org/10.1021/ja207931r | J. Am. Chem.Soc. 2012, 134, 1600–1605

and this likely results from some delocalization of the excited electron. This view of a less localized electron at the site of the metal ion is indeed perfectly corroborated by our measurements. From Figure 3A (inset) we know that the t_{2g} levels energetically overlap with the lowest-BE orbital ($1b_1$) of water, leading to orbital mixing. Such a stabilized excited t_{2g}-electron will be unlikely to refill the 2p hole within the core-hole lifetime, and this leads to a signal decrease in the lower-kinetic-energy part of the Auger spectrum (lowest amount of energy to be gained in the core-hole refill). This is exactly what we find in the spectra, i.e., a reduced signal enhancement at the onset of Auger-electron emission. As we have mentioned earlier in this work, the reduction of peak (a) in the PEY has the same origin for the disappearance of this peak in the TFY and, accordingly, explains its nonradiative behavior. Only for high enough excitation energy, sufficient to populate one of the e_g states, where there is no overlap with the energies of water, will the excited electron promptly refill the 2p hole. This is nicely reflected by the fact that the high-energy peaks (peaks (f) and beyond) are in a good agreement for all three XA modes.

■ CONCLUSIONS

By core and valence (photo)electron-spectroscopy measurements from cobalt-chloride aqueous solution, we observe metal-to-ligand charge transfer connected with the strong metal−water orbital overlap. This finding is fully based on experimental grounds. On the basis of electron binding energies, and specifically from matching valence energies of water valence bands and some metal 3d-derived levels, together with the resonant-enhanced valence PE signal, we directly monitor the quenching of the 2p core-hole refill. Such state-specific (ultrafast) relaxation behavior can explain the spectral differences, obtained in our comparative transmission, fluorescence, and electron-detecting X-ray absorption measurements. We have shown that RPE spectroscopy is very sensitive to the exact nature of the electronic-structure interactions of a given transition-metal aqueous solution. It is thus expected that we can use RPE for the systematic study of transient hybridization and associated charge transfer, for instance as a function of ion oxidation state. The present work marks a significant step forward toward understanding X-ray absorption spectra from transition-metal aqueous solutions, and we believe that we have laid here the groundwork for many XA measurements from transition metal ions in an aqueous environment (including biological systems) to follow.

■ ASSOCIATED CONTENT

Ⓢ Supporting Information

Detailed explanation and parameters of the XA-spectrum calculation in the framework of the ligand field multiplet (LFM) model. This material is available free of charge via the Internet at http://pubs.acs.org.

■ AUTHOR INFORMATION

Corresponding Author

bernd.winter@helmholtz-berlin.de; emad.aziz@helmholtz-berlin.de

■ ACKNOWLEDGMENTS

The authors gratefully acknowledge assistance from the BESSY staff. E.F.A. acknowledges support from the Helmholtz-Gemeinschaft via the Young Investigator Fund VHNG-635 and the European Research Council Grant No. 279344, and B.W. thanks the Deutsche Forschungsgemeinschaft (project WI 1327/3-1) for support.

■ REFERENCES

(1) Aziz, E. F.; Rittmann-Frank, M. H.; Lange, K. M.; Bonhommeau, S.; Chergui, M. *Nature Chem.* **2010**, *2*, 853.
(2) Bauer, M.; Stalinski, T.; Aziz, E. F. *ChemPhysChem* **2011**, *12*, 2088.
(3) Aziz, E. F.; Eisebitt, S.; de Groot, F.; Chiou, J. W.; Dong, C. G.; Guo, J. H.; Eberhardt, W. *J. Phys. Chem. B* **2007**, *111*, 4440.
(4) de Groot, F. *Coord. Chem. Rev.* **2005**, *249*, 31.
(5) de Groot, F.; Kotani, A. *Core level spectroscopy of solids*; CRC: Boca Raton, FL, 2008.
(6) Hergenhahn, U. *J. Electron Spectrosc.* **2011**, *184*, 78.
(7) Schwartz, C. P.; Fatehi, S.; Saykally, R. J.; Prendergast, D. *Phys. Rev. Lett.* **2010**, *105*, 198102.
(8) Thürmer, S.; Seidel, R.; Eberhardt, W.; Bradforth, S. E.; Winter, B. *J. Am. Chem. Soc.* **2011**, *133*, 12528.
(9) Seidel, R.; Thurmer, S.; Winter, B. *J. Phys. Chem. Lett.* **2011**, *2*, 633.
(10) Winter, B.; Aziz, E. F.; Hergenhahn, U.; Faubel, M.; Hertel, I. V. *J. Chem. Phys.* **2007**, *126*, 124504.
(11) Aziz, E. F. *J. Electron Spectrosc.* **2010**, *177*, 168.
(12) Aziz, E. F.; Ottosson, N.; Bonhommeau, S.; Bergmann, N.; Eberhardt, W.; Chergui, M. *Phys. Rev. Lett.* **2009**, *102*, 068103.
(13) Winter, B. *Nucl. Instrum. Methods A* **2009**, *601*, 139.
(14) Lange, K. M.; Konnecke, R.; Ghadimi, S.; Golnak, R.; Soldatov, M. A.; Hodeck, K. F.; Soldatov, A.; Aziz, E. F. *Chem. Phys.* **2010**, *377*, 1.
(15) Lewis, T.; Faubel, M.; Winter, B.; Hemminger, J. C. *Angew. Chem., Int. Ed.* **2011**, *50*, 10178.
(16) Lewis, T.; Winter, B.; Stern, A. C.; Baer, M. D.; Mundy, C. J.; Tobias, D. J.; Hemminger, J. C. *J. Phys. Chem. C* **2011**, *115*, 21183.
(17) Aziz, E. F.; Zimina, A.; Freiwald, M.; Eisebitt, S.; Eberhardt, W. *J. Chem. Phys.* **2006**, *124*, 114502.
(18) Ohno, M.; van Riessen, G. A. *J. Electron Spectrosc.* **2003**, *128*, 1.
(19) Winter, B.; Weber, R.; Widdra, W.; Dittmar, M.; Faubel, M.; Hertel, I. V. *J. Phys. Chem. A* **2004**, *108*, 2625.
(20) Naslund, L. A.; Cavalleri, M.; Ogasawara, H.; Nilsson, A.; Pettersson, L. G. M.; Wernet, P.; Edwards, D. C.; Sandstrom, M.; Myneni, S. *J. Phys. Chem. A* **2003**, *107*, 6869.
(21) Kim, K. S. *Phys. Rev. B* **1975**, *11*, 2177.
(22) Shen, Z. X.; Allen, J. W.; Lindberg, P. A. P.; Dessau, D. S.; Wells, B. O.; Borg, A.; Ellis, W.; Kang, J. S.; Oh, S. J.; Lindau, I.; Spicer, W. E. *Phys. Rev. B* **1990**, *42*, 1817.